SUPPLEMENTARY INFORMATION **Campbell and Desai**

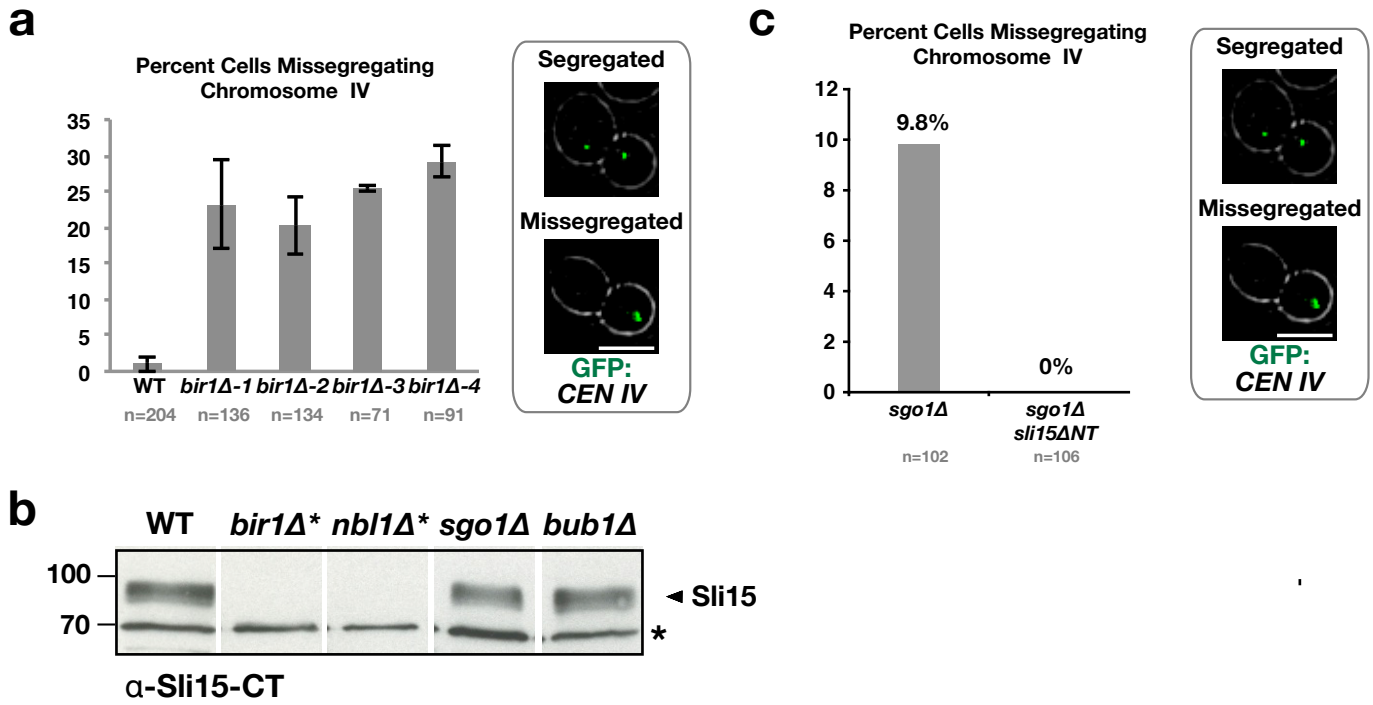

Supplementary Figure 1. Characterization of deletions of proteins that target the CPC to chromatin.
(**a**) Analysis of segregation fidelity of GFP-tagged chromosome IV in independent *bir1Δ** isolates. Images on the right show examples of properly segregated and missegregated chromosome IV (scale bar is 5 μm). The average of 3 to 5 experiments is shown; error bars represent standard error.
(**b**) Immunoblot of extracts prepared from strains with deletions in genes required for chromosomal targeting of the CPC probed with an antibody raised against the C-terminus of Sli15. Although Sli15 appears destabilized in *bir1Δ** and *nbl1Δ** cells, *sgo1Δ* and *bub1Δ* do not affect Sli15 protein levels. The asterisk (*) indicates a non-specific band recognized by the primary antibody that serves as a loading control. The lanes are from different parts of the same gel.
(**c**) Analysis of segregation fidelity of GFP-tagged chromosome IV in cells of the indicated genotypes. Images on the right show examples of properly segregated and missegregated chromosome IV (scale bar is 5 μm).

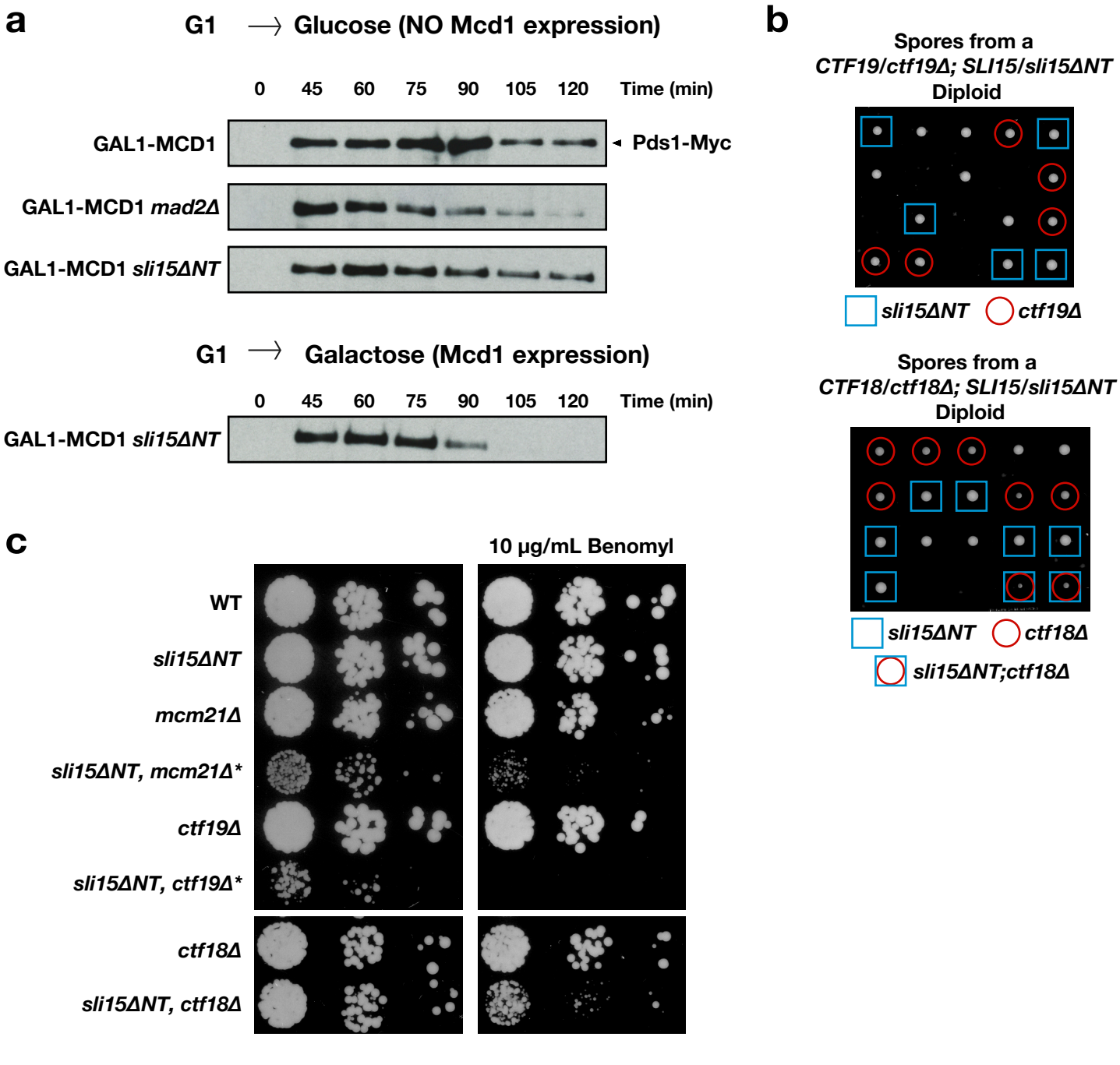

Supplementary Figure 2. *sli15ΔNT* signals loss of tension to the spindle checkpoint and is synthetically lethal/sick with genes implicated in cohesion.
(**a**) Assay for the activation of the spindle checkpoint upon removal of cohesion by Mcd1 depletion. The cell cycle delay requires CPC-dependent sensing of a lack of tension.
(**b**) Tetrad dissections showing synthetic lethality/sickness of *sli15ΔNT* with *ctf19Δ* and *ctf18Δ*.
(**c**) Compromised growth and benomyl sensitivity of the *sli15ΔNT* mutation combined with *mcm21Δ*, *ctf19Δ* or *ctf18Δ*. Rare survivors of *mcm21Δ*;*sli15ΔNT* and *ctf19Δ*;*sli15ΔNT* double mutants are observed after extended growth.

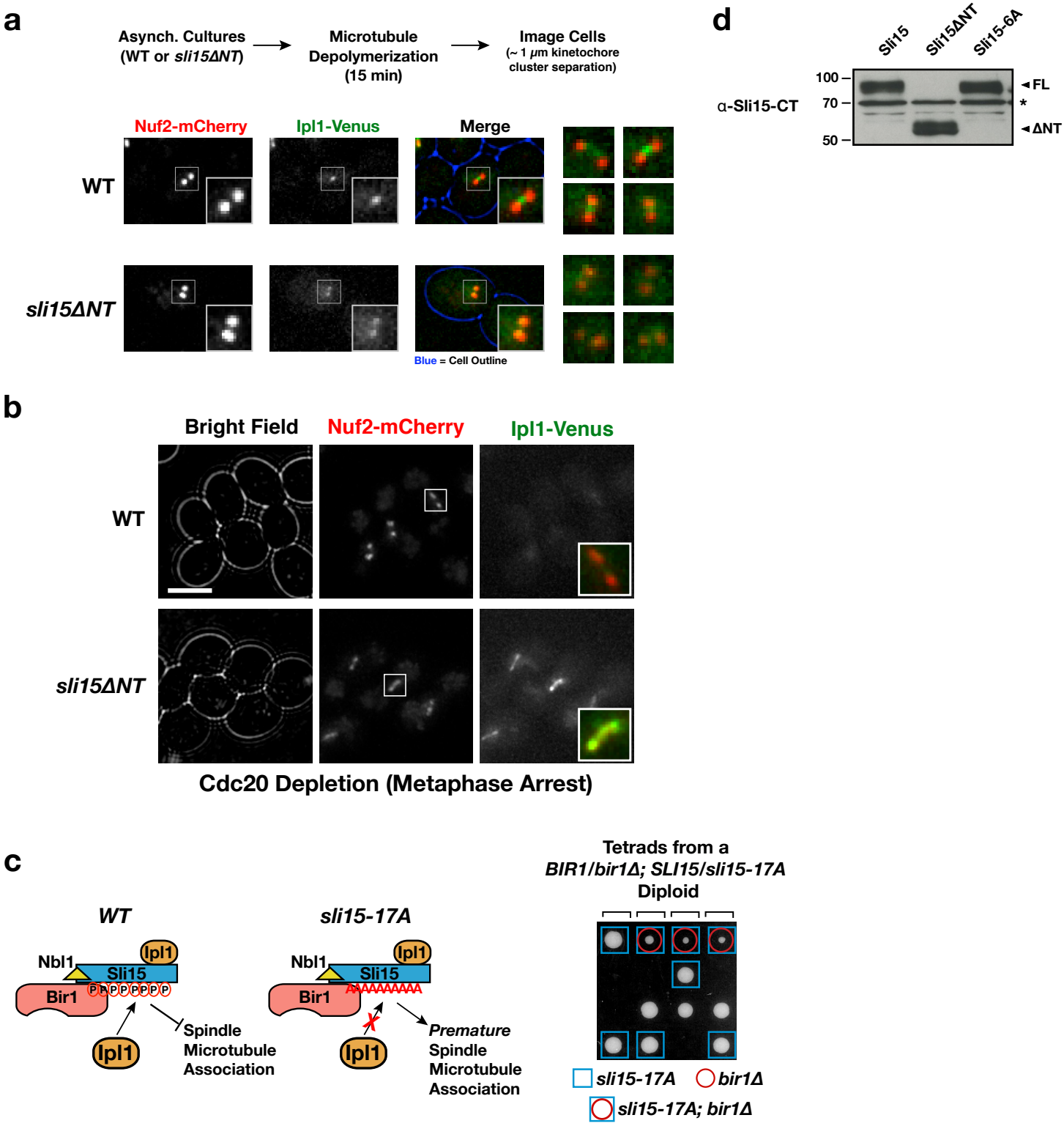

Supplementary Figure 3. Change in Ipl1 localization with *sli15ΔNT* and suppression of *bir1Δ* by *sli15-17A*.
(**a**) Images of cells expressing Nuf2-mCherry and Ipl1-Venus in the presence of either Sli15 or Sli15ΔNT after brief microtubule depolymerization. A cell with ~1 μm separation of Nuf2-mCherry clusters is shown for each. Boxes are 2.1 μm square. 4 additional examples of merged mCherry & Venus signals are shown on the right.
(**b**) Images of cells arrested in metaphase by Cdc20 depletion expressing Nuf2-mCherry and Ipl1-Venus with either Sli15 or Sli15ΔNT. Scale bar is 5 μm; merged insets are magnified 2.5-fold.
(**c**) Schematic summarizing prior work on Ipl1 regulation of Sli15 microtubule binding and tetrad analysis showing growth of sli15-17A;bir1Δ double mutant cells.
(**d**) Immnublot of extracts prepared from strains expressing either wild type Sli15, Sli15ΔNT or Sli15-6A using an antibody raised against the C-terminus of Sli15. The asterisk (*) indicates a non-specific band recognized by the primary antibody that serves as a loading control. The first two lanes are the same as in Figure 2c.

Supplementary Table 1. Plasmids and Yeast Strains used in this study.

Strain	Genotype	Source	Background	Figure(s)
ODY48	*MATα trp1Δ63 ura3-52 his3Δ200*	b	S288C	2b, 3b
ODY49	*MATa trp1Δ63 ura3-52 his3Δ200*	a	S288C	2c, 2f, 2g, 2h, 3c, S1b, S2c
ODY50	*MATα/MATa trp1Δ63 ura3-52 his3Δ200*	b	S288C	
ODY205	ODY50 + *BIR1/bir1Δ::hphNT1*	b	S288C	1b
ODY206	ODY50 + *SLI15/sli15Δ::TRP1* pOD594*::URA3*	b	S288C	1c
ODY207	ODY50 + *SLI15/sli15Δ::TRP1* pOD1254*::URA3*	b	S288C	1c
ODY208	ODY50 + *SLI15/sli15Δ::TRP1* pOD1255*::URA3*	b	S288C	1c
ODY209	ODY50 + *SLI15/sli15Δ::TRP1* pOD1256*::URA3*	b	S288C	1c
ODY210	ODY50 + *SLI15/sli15Δ::TRP1* pOD1257*::URA3*	b	S288C	1c
ODY211	ODY50 + *SLI15/sli15Δ::TRP1* pOD1258*::URA3*	b	S288C	1c
ODY212	ODY50 + *SLI15/sli15Δ::TRP1* pOD1259*::URA3*	b	S288C	1c
ODY213	ODY50 + *SLI15/sli15Δ2-228::kanMX4*	b	S288C	1c
ODY214	ODY49 + *SLI15-6HA::natNT2*	b	S288C	1d
ODY215	ODY49 + *SLI15-6HA::natNT2 BIR1-9Myc::hphNT1*	b	S288C	1d
ODY216	ODY49 + *sli15Δ2-228-6HA::natNT2 BIR1-9Myc::hphNT1*	b	S288C	1d
ODY217	ODY48 + *IPL1-Venus::kanMX4 NUF2-mCherry::hphMX4*	b	S288C	1f, S3a
ODY218	ODY49 + *IPL1-Venus::kanMX4 NUF2-mCherry::hphMX4 sli15Δ2-228*	b	S288C	1f, S3a
ODY219	ODY49 + *BIR1-Venus::kanMX4 NUF2-mCherry::hphMX4*	b	S288C	1f
ODY220	ODY49 + *BIR1-Venus::kanMX4 NUF2-mCherry::hphMX4 sli15Δ2-228*	b	S288C	1f
ODY221	ODY49 + *NBL1-Venus::kanMX4*	b	S288C	1f
ODY222	ODY49 + *NBL1-Venus::kanMX4 sli15Δ2-228*	b	S288C	1f
ODY223	ODY50 + *BIR1/bir1Δ::hphNT1 SLI15/sli15Δ2-228::kanMX4*	b	S288C	2a
ODY224	ODY49 + *sli15Δ2-228*	b	S288C	2b, 2c, 2f, 2g, 2h, 3b, 3c, S2c
ODY225	ODY48 + *SLI15::kanMX4 bir1Δ::hphNT1*	b	S288C	2b, S1b
ODY226	ODY49 + *sli15Δ2-228::kanMX4 bir1Δ::hphNT1*	b	S288C	2b
ODY227	ODY49 + *SLI15::kanMX4 nbl1Δ::hphNT1*	b	S288C	2b, S1b
ODY228	ODY49 + *sli15Δ2-228::kanMX4 nbl1Δ::hphNT1*	b	S288C	2b
ODY229	ODY49 + *bir1Δ::hphNT1*	b	S288C	2f
ODY230	ODY49 + *sli15Δ2-228::kanMX4 bir1Δ::hphNT1*	b	S288C	2f
SBY213	*MATa ura3-1 leu2,3-112 his3-11::pCUP1-GFP12-lacI12::HIS3 trp1-1::256lacO::TRP1 lys2Δ ade2-1 can1-100 bar1Δ*	a	W303	2d, S1a
ODY232	SBY213 + *sli15Δ2-228*	b	W303	2d
ODY233	SBY213 + *bir1Δ::hphNT1*	b	W303	2d, S1a
ODY234	SBY213 + *bir1Δ::hphNT1*	b	W303	2d, S1a
ODY235	SBY213 + *bir1Δ::hphNT1*	b	W303	2d, S1a
ODY236	SBY213 + *bir1Δ::hphNT1*	b	W303	2d, S1a
ODY237	SBY213 + *bir1Δ::hphNT1*	b	W303	2d, S1a
ODY238	SBY213 + *bir1Δ::hphNT1 sli15Δ2-228*	b	W303	2d
ODY239	ODY48 + *mad1Δ::hphNT1*	b	S288C	2g
ODY240	ODY49 + *mad1Δ::hphNT1*	b	S288C	2h, 3c

ODY241	ODY49 + *mad1Δ::hphNT1 sli15Δ2-228::kanMX4*	b	S288C	2h, 3c
ODY242	ODY49 + *sli15-3*	b	S288C	2h
ODY243	ODY49 + *mad1Δ::hphNT1 sli15-3*	b	S288C	2h
Y726	*MATa ura3*::pAFS152[*URA3 PCYC-GFP-lacI*] *trp1-Δ63 his3-1 leu2* l*ys2*::pMDE798[*PDMC1-GFP-lacI*] *tyr1-2 met13-c cyh2-1* pMDE1145 [*SPC42-DSRed*] *CEN1*::pJN2[*lacO256 LEU2*]	c	MDY431	
X764	*MATα ura3*::pAFS152[*URA3 PCYC-GFP-lacI*] *trp1-63 his3-1 leu2 met13-d tyr1-1 can1-R lys2*::pMDE798[*PDMC1-GFP-lacI*] *CEN1*::pJN2[*lacO256 LEU2*]	c	MDY433	
ODY246	X764 + *sli15Δ::kanMX4* pOD1260[*SLI15::HIS3*]	b	MDY433	
ODY247	Y726 + *sli15Δ::hphNT1* pOD1260[*SLI15::HIS3*]	b	MDY431	
ODY248	Y726 + *sli15Δ::hphNT1* pOD1261[*sli15Δ2-228::HIS3*]	b	MDY431	
ODY249	X764 + *sli15Δ::natNT2* pOD1261[*sli15Δ2-228::HIS3*]	b	MDY433	
ODY250	ODY246 x ODY247	b		2i
ODY251	ODY249 x ODY247	b		2i
ODY252	ODY246 x ODY248	b		2i
ODY253	ODY249 x ODY248	b		2i
ODY254	ODY48 + *SLI15::kanMX4 sgo1Δ::hphNT1*	b	S288C	3b
ODY255	ODY49 + *sli15Δ2-228::kanMX4 sgo1Δ::hphNT1*	b	S288C	3b
ODY256	ODY48 + *SLI15::kanMX4 bub1Δ::hphNT1*	b	S288C	3b, S1b
ODY257	ODY49 + *sli15Δ2-228::kanMX4 bub1Δ::hphNT1*	b	S288C	3b
ODY258	ODY49 + *sgo1Δ::hphNT1*	b	S288C	3c, S1b
ODY259	ODY49 + *sli15Δ2-228::kanMX4 sgo1Δ::hphNT1*	b	S288C	3c
ODY260	ODY50 + *MCM21/mcm21Δ::hphNT1 SLI15/sli15Δ2-228::kanMX4*	b	S288C	3e
ODY261	ODY48 + *SLI15-Venus::kanMX4 NUF2-mCherry::hphMX4*	b	S288C	1e, 4a
ODY262	ODY48 + *sli15Δ2-228-Venus::kanMX4 NUF2-mCherry::hphMX4*	b	S288C	1e, 4a
ODY263	ODY48 + *SLI15-Venus::kanMX4 NUF2-mCherry::hphMX4 PGAL1-3HA-CDC20::TRP1*	b	S288C	4b
ODY264	ODY48 + *sli15Δ2-228-Venus::kanMX4 NUF2-mCherry::hphMX4 PGAL1-3HA-CDC20::TRP1*	b	S288C	4b
ODY265	ODY48 + *IPL1-Venus::kanMX4 NUF2-mCherry::hphMX4 PGAL1-3HA-CDC20::TRP1*	b	S288C	S3b
ODY266	ODY48 + *sli15Δ2-228 IPL1-Venus::kanMX4 NUF2-mCherry::hphMX4 PGAL1-3HA-CDC20::TRP1*	b	S288C	S3b
ODY267	ODY50 + *BIR1/bir1Δ::hphNT1 SLI15::kanMX4/sli15-6A*	b	S288C	4c
ODY268	ODY50 + *CTF19/ctf19Δ::hphNT1 SLI15/sli15Δ2-228::kanMX4*	b	S288C	S2b
ODY269	ODY50 + *CTF18/ctf18Δ::hphNT1 SLI15/sli15Δ2-228::kanMX4*	b	S288C	S2b
ODY270	ODY48 + *mcm21Δ::hphNT1*	b	S288C	S2c
ODY271	ODY48 + *sli15Δ2-228::kanMX4 mcm21Δ::hphNT1*	b	S288C	S2c
ODY272	ODY48 + *ctf19Δ::hphNT1*	b	S288C	S2c
ODY273	ODY48 + *sli15Δ2-228::kanMX4 ctf19Δ::hphNT1*	b	S288C	S2c
ODY274	ODY48 + *ctf18Δ::hphNT1*	b	S288C	S2c
ODY275	ODY48 + *sli15Δ2-228::kanMX4 ctf18Δ::hphNT1*	b	S288C	S2c
ODY276	ODY50 + *BIR1/bir1Δ::hphNT1 SLI15::kanMX4/sli15-17A*	b	S288C	S3c
ODY277	ODY50 + *alk2Δ::natNT2 alk1Δ::hphNT1 sli15Δ2-228::kanMX4*	b	S288C	3d
ODY278	*ura3-52 lys2-801 ade2-101 his3Δ200 trp1-Δ63 leu2-Δ1* CFIII*(HIS3 SUP11)*	d	S288C	2e
ODY279	ODY278 + *sli15Δ2-228*	b	S288C	2e
ODY280	ODY278 + *mcm21Δ::hphNT1*	b	S288C	2e
SBY4820	*ura3-1 leu2-3,112 his3-11* pCUP1-GFP-*lacI*::*HIS3 trp1-1* 256*lacO*::*TRP1 lys2Δ can1-100 bar1-1 PDS1-18MYC::LEU2 ade2-1 PGAL-3HA-MCD1::KAN*	e	W303	S2a

SBY4821	SBY4820 + *mad2Δ::KAN*	e	W303	S2a
ODY283	SBY4820 + *sli15Δ2-228*	b	W303	S2a
ODY284	SBY213 + *sgo1Δ::hphNT1*	b	W303	S1c
ODY285	SBY213 + *sgo1Δ::hphNT1 sli15Δ2-228*	b	W303	S1c
ODY288	ODY49 + *sli15-6A*	b	S288C	S3d
Plasmid	**Description**	**Source**		
pRS306	pBluescript URA3	f		
pOD594	Sli15 + 1kB Upstream in pRS306	a		
pOD1254	*sli15Δ2-20* + 1kB Upstream in pRS306	b		
pOD1255	*sli15Δ2-100* + 1kB Upstream in pRS306	b		
pOD1256	*sli15Δ2-228* + 1kB Upstream in pRS306	b		
pOD1257	*sli15Δ2-300* + 1kB Upstream in pRS306	b		
pOD1258	*sli15Δ2-400* + 1kB Upstream in pRS306	b		
pOD1259	*sli15Δ228-300* + 1kB Upstream in pRS306	b		
pRS303	pBluescript HIS3			
pOD1260	Sli15 + 1kB Upstream in pRS303	b		
pOD1261	*sli15Δ2-228* + 1kB Upstream in pRS303	b		

a. Sandall et. al 2006
b. This study
c. Dean Dawson's Laboratory
d. Phil Hieter's Laboratory
e. Sue Biggins' Laboratory
f. Sinorski and Hieter *Genetics* **122:** 19-27 (1989)

SUPPLEMENTARY DISCUSSION

One question that emerges from our results is why the *sli15ΔNT* mutant is viable whereas *bir1Δ* cells are not. We show that, as in human and chicken cells[31,32], yeast Sli15 is destabilized in the absence of Bir1 (**Fig. S1b**); removing the N-terminal region of Sli15 must prevent this destabilization as deletion of *BIR1* has no effect in *sli15ΔNT* cells (**Fig. 2a,b**). However, protein stability does not explain the rescue of *sgo1Δ* and *bub1Δ* phenotypes by *sli15ΔNT*, as neither of these deletions affects the levels of Sli15 (**Fig. S1b**). Instead rescue of *sgo1Δ* and *bub1Δ* is likely explained by premature clustering of Sli15ΔNT on the metaphase spindle (**Fig. 4b**). The basis behind this premature spindle localization is unclear, but may involve a reduction in Sli15ΔNT phosphorylation by Cdk1 and/or Ipl1 (note that all 6 Cdk1 sites and 15 of 17 Ipl1 phosphorylation sites suggested to control spindle microtubule localization are still present in the Sli15ΔNT protein). We therefore suggest that Sli15ΔNT functions in the complete absence of Bir1 due to stabilization of the truncated protein in combination with its premature clustering on the spindle.

Since the results presented here indicate that the inner centromere localization of the CPC is not required for chromosome biorientation, why is that localization widely conserved? The synthetic lethality of *sli15ΔNT* observed with *mcm21Δ, ctf19Δ* or *ctf18Δ* (**Fig. 3e; S2b,c**) points to a role for chromatin-localized CPC in cohesion establishment or maintenance. A minor defect in sister chromatid cohesion could also potentially explain the slight increase in missegregation observed in *sli15ΔNT* cells (**Fig. 2e**). Alternatively, as *S. cerevisiae* does not exhibit merotely (a single kinetochore attaching to two spindle poles), the correction of merotelic attachments may be the primary function of inner centromere-localized CPC[33,34].

We observed localization of Sli15 and Ipl1 between sister kinetochore clusters after microtubule depolymerization but not in metaphase-arrested cells with intact spindles (**Fig. 4a**). One trivial explanation for the localization observed following microtubule depolymerization is binding to residual microtubules that persist after drug treatment. This explanation is unlikely because Sli15ΔNT, which exhibits robust and premature spindle microtubule localization (**Fig. 4b; Fig. 1e**), does not localize between sister kinetochore clusters following microtubule depolymerization (**Fig. 4a**). Instead, we believe these observations indicate enrichment of the CPC at the inner centromere upon microtubule depolymerization. Enrichment of the CPC at the inner centromere has also been reported on misaligned and unattached chromosomes in diploid human cells[35]. These observations suggest the existence of a conserved feedback mechanism between the bioriented state and inner centromere CPC localization, in which there is a decrease in inner centromere localization following proper biorientation. Understanding the mechanism underlying this feedback could prove instrumental in determining the function(s) of the CPC localized at the inner centromere.

For simplicity, our model depicts activated Ipl1/Aurora B acting alone at the kinetochore (**Fig. 4d**). However, Sli15 may likely continue to play a role at this stage. The central region of Sli15 that contains microtubule-binding activity is essential even in the presence of the Bir1/Nbl1 interacting N-terminus (**Fig. 1c** & [36]). Since localization to the inner centromere should be sufficient to cluster the kinase, this finding suggest that there is an additional essential role of the central region of Sli15 that may or may not involve its ability to bind to microtubules.

The weak localization of Sli15ΔNT coincident with kinetochore clusters following microtubule depolymerization (**Fig. 4a**) is intriguing. Possible sources of this localization include residual kinetochore microtubules (between each kinetochore cluster and its adjacent spindle pole) or concentration on Ipl1 substrates at the kinetochore. A more interesting possibility is that this

weak kinetochore localization may reflect a kinetochore-binding site for active Ipl1-Sli15ΔNT complex (as suggested by Deluca et al.[37]). Exposure of such a binding site specifically when kinetochores are not under tension would provide a straightforward mechanism for tension sensing by the CPC. Elucidation of the basis for this localization and its functional significance will be an important goal of future work.

31. Honda, R., Körner, R. & Nigg, E. A. Exploring the functional interactions between Aurora B, INCENP, and survivin in mitosis. *Mol Biol Cell* **14**, 3325–3341 (2003).
32. Yue, Z. *et al.* Deconstructing Survivin: comprehensive genetic analysis of Survivin function by conditional knockout in a vertebrate cell line. *J Cell Biol* **183**, 279–296 (2008).
33. Knowlton, A. L., Lan, W. & Stukenberg, P. T. Aurora B is enriched at merotelic attachment sites, where it regulates MCAK. *Curr Biol* **16**, 1705–1710 (2006).
34. Cimini, D., Wan, X., Hirel, C. B. & Salmon, E. D. Aurora kinase promotes turnover of kinetochore microtubules to reduce chromosome segregation errors. *Curr Biol* **16**, 1711–1718 (2006).
35. Salimian, K. J. *et al.* Feedback control in sensing chromosome biorientation by the Aurora B kinase. *Curr Biol* **21**, 1158–1165 (2011).
36. Sandall, S. *et al.* A Bir1-Sli15 complex connects centromeres to microtubules and is required to sense kinetochore tension. *Cell* **127**, 1179–1191 (2006).
37. DeLuca, K. F., Lens, S. M. A. & DeLuca, J. G. Temporal changes in Hec1 phosphorylation control kinetochore-microtubule attachment stability during mitosis. *J Cell Sci* **124**, 622–634 (2011).